# Rapid Hybrid Acquisition of Ultra-Wideband Signals

Honglei Zhang, Shuangqing Wei, Dennis L. Goeckel, and Moe Z. Win

March 31, 2005

**Abstract**

Impulsive ultra-wideband (UWB) radio provides many promising features for wireless communications in a dense multipath environment. However, these features are largely the result of the enormous effective processing gain, which can make acquisition difficult at the receiver. In this paper, a recently developed theory of minimum complexity sequential detection is applied to the hybrid acquisition problem. As in previous hybrid schemes, a number of potential timing phases are checked as a group; however, a phase is disregarded as soon as it appears unlikely rather than waiting for a "winner" to be chosen from the group. Another phase then replaces the disregarded one. Analysis and simulation results indicate that the proposed scheme can improve average acquisition times for highly spread systems operating over either additive white Gaussian noise (AWGN) or multipath fading channels.

Honglei Zhang, Dennis Goeckel
ECE Department
University of Massachusetts
100 Natural Resources Rd
Amherst, MA 01003-9292
Tel:(413) 545-3514
Fax:(413) 545-4611
Email: {hlzhang,goeckel}@ecs.umass.edu

Shuangqing Wei
ECE Department
Louisiana State University
Baton Rouge, LA 70803
Tel:(225) 578-5536
Fax: (225) 578-5520
Email: swei@ece.lsu.edu

Moe Win
LIDS
MIT
Cambridge, MA 02139
Tel: (617) 253-9341
Fax: (617) 253-3578
moewin@mit.edu

# 1 Introduction

Ultra-wideband (UWB) radio schemes have a number of potential advantages that arise from the enormous bandwidth of the signal. From a co-existence standpoint, such systems can spread their energy so finely across a broad frequency range as to cause little interference in the operating band of most existing narrowband systems; hence, the Federal Communications Commission (FCC) of the United States has approved limited unlicensed use of UWB systems [1]. From a reliability standpoint, the large bandwidth implies that the transmitted signal will provide enormous frequency diversity against multipath fading, which can then be mitigated by proper receiver design. Finally, from a data rate standpoint, the large bandwidth implies the potential to carry much higher data rates than conventional systems, and hence one of the oft-discussed application areas of UWB is in so-called "wireless USB" [2].

However, the large bandwidth of UWB systems can also make system design very difficult. From a theoretical perspective, recent results have shown that, although the inherent capacity of the wideband multipath fading channel is equal asymptotically to that of the AWGN channel [3], the achievement of such capacity requires "peaky" signals, and the capacity of systems which spread their energy very finely in the frequency domain, as in the typically envisioned and FCC-approved UWB systems, diminishes to zero in the limit of large bandwidth [4, 5]. The reason for this (perhaps counterintuitive) result is that channel estimation becomes very difficult as the number of resolvable signal paths that need to be estimated grows to infinity.

Although the studies mentioned in the previous paragraph are largely theoretical, implementation problems due to the large bandwidth, or, equivalently, the extremely short pulse (or chip) duration, have slowed the development of practical UWB systems. In particular, the short pulse makes the acquisition of the code and frame timing extremely difficult, and such acquisition, as with many spread-spectrum systems, can limit overall system performance [6, 7]. Practical channel estimation can indeed be difficult, and, even *given* accurate channel estimation, the standard UWB system requires a rake receiver with a large number of fingers and thus of prohibitive complexity [8]. These two problems, which are exacerbated by the inability to digitize the entire communication bandwidth as required by many proposed algorithms, have been part of the motivation for the recent migration of much of industry away from true single-channel impulse radio to a multiband approach, where the bandwidth of each band carrying a multicarrier signal is set to 500 MHz [2] - the minimum allowable by the FCC.

In this paper, the timing acquisition problem is addressed. In particular, the focus is on acquisition in the more "classical" forms of UWB: impulse radio with time hopping [9], or extremely wideband direct-sequence (DS) code-division multiple-access (CDMA) [10]. In each case, the goal is to achieve frame and spreading code acquisition. The acquisition process can be viewed as one in which the initial time uncertainty $T_{unc}$ is reduced to an interval on the order of the time resolution $T_{res}$ of the signal. In the classical UWB systems of interest, $T_{unc}$ is the spreading code repetition period and $T_{res}$ is approximately the inverse of the bandwidth of the signal. Hence, the number $\frac{T_{unc}}{T_{res}}$ of possible timing phases to be checked can be enormous, and, thus, the acquisition process can severely limit overall system performance [11].

Acquisition in highly spread communication systems is generally based around a receiver with some number of analog or digital correlators; in the UWB case, these are generally analog correlators. Each of these calculates the partial correlation of a small portion of the actual received signal with the anticipated received signal given a certain hypothesized code and frame timing phase. As time progresses, the window over which this partial correlation is performed grows until it is determined that some decision can be made. If a correlator output has become large enough, the hypothesized code and frame timing phase which corresponds to that correlator is declared as correct, and the acquisition scheme enters a verification stage to check that decision. If none of the correlator outputs look promising, the receiver discards all of the hypothesized code and frame timings currently under consideration and brings in a new set of timing phases for consideration. This process continues until the correct hypothesis is found.

There are many different methods for performing this acquisition, and each selects a point on the performance versus complexity tradeoff curve. At one extreme are serial acquisition schemes, which employ only a single correlator, and, hence, only check a single timing phase at a time. Whereas serial schemes are extremely simple (only a single correlator), the average acquisition time can be very large in highly spread systems, since the correlator will generally have to check and discard many phases before the correct timing phase is found. At the other extreme are parallel acquisition schemes, which have a correlator for each of the possible frame and code timings. In this case, acquisition is generally rapid - the system is simply run until the output of one of the correlators dominates all of the rest; however, the circuit complexity to support such a large number of correlators is generally prohibitive, particularly in highly spread systems.

Since serious drawbacks exist with both the serial and parallel schemes for highly spread systems, a hybrid acquisition scheme is generally favored. In a hybrid scheme, the system attempts to strike a balance between performance and complexity by employing $M-1$ correlators, where $M-1$ is some small number relative to the total number of possible timing phases. A general structure of hybrid acquisition schemes is shown in Figure 1. All possible timing phases are divided into a number of groups. Each group contains $M-1$ phases, and $M-1$ correlators are applied to test these $M-1$ phases. Thus, the testing stage corresponds to an $M$-ary hypothesis testing problem - a null hypothesis, which corresponds to the decision that none of the $M-1$ phases currently under consideration is correct, and $M-1$ timing phase hypotheses, each of which corresponds to deciding that a particular timing phase is correct. If the null hypothesis is selected, the $M-1$ timing phases currently under consideration are discarded, and a new set of $M-1$ hypotheses is placed under consideration; if one of the $M-1$ timing phase hypotheses is selected, this hypothesis will be checked in the verification stage. If it fails the verification stage, the testing stage will move onto a new group of $M-1$ phases, as if the null hypothesis had been chosen.

The method for deciding among the $M$ hypotheses is a critical component of the algorithm. In the most classical of approaches, each group of $M$ hypotheses is tested by first collecting some fixed number of samples and then deciding which of the hypotheses is correct. Such a test is termed a fixed sample size (FSS) test. However, each $M$-ary hypothesis testing problem can also be structured as a sequential detection problem. In other words, as each new sample arrives during the testing of a given set of hypotheses, the receiver decides whether it has observed enough information to reliably choose a hypothesis or whether it should collect more samples. Although sequential detection schemes are generally more complicated to implement than fixed sample size tests, average decision times can generally be reduced by a factor of 2-3 [12].

Because of the efficiency of sequential detection, it has taken on a prominent role in acquisition schemes. In particular, each advance in sequential detection generally leads to an advance in acquisition in highly spread systems. The most recent prior example was the application of the $M$-ary sequential probability ratio test (MSPRT) [13] to the hybrid acquisition problem [6], where it was observed that the MSPRT greatly reduces the expected acquisition time versus FSS tests.

In [14, 15], the authors proposed a modified MSPRT technique termed the reduced-complexity sequential probability ratio test (RC-SPRT). The main philosophy of this novel test, as described in detail later in this paper, is to remove *individual* hypotheses from consideration in the $M$-ary test as they become very unlikely, rather than waiting until $M-1$ hypotheses are effectively simultaneously removed when a decision on the group is made. The RC-SPRT can reduce the overall complexity in that it minimizes the expected aggregate number of hypotheses tested, which is the appropriate metric for applications where each hypothesis tested at a given stage contributes to the complexity cost. Motivated by the work in [14, 15], the RC-SPRT is applied in this paper to the testing stage in hybrid acquisition schemes. During the test of a given group of $M-1$ timing phases, unlikely phases are removed immediately upon becoming unlikely instead of waiting for one hypothesis to be chosen. Rather than leaving the corresponding correlator idle, as may be suggested by the original RC-SPRT, a new test phase is assigned to the correlator and the $M$-ary hypothesis test continues. Hence, instead of waiting to make a decision on the entire group and then discarding $M-1$ timing phases simultaneously as in previous tests, this new test will immediately remove any timing phase that appears unlikely and replace it with a new one. In essence, the goal is to translate the complexity savings of the RC-SPRT [14, 15] into savings in expected acquisition time.

Due to the highly spread nature of the impulsive UWB system, which requires a simulation that has a sample time (generally, sub-nanosecond) that can be many orders of magnitude smaller than the symbol period, it is difficult to run extensive simulations. This motivates an accurate analysis of the proposed acquisition scheme. The analysis of the proposed scheme is complicated due to the complexity of the proposed hypothesis tests; however, through a combination of a state-spaced approach and parameters for such obtained through much simpler simulations, the expected acquisition time of the proposed approach can be approximated.

This paper is organized as follows. Section 2 describes the models for both a direct-sequence spread spectrum (DS/SS) system and an impulse radio system. Section 3 describes the proposed algorithm, and Section 4 gives the analysis of such. Finally, Section 5 presents the numerical results and Section 6 the conclusions.

# 2 System Models and Associated Hypotheses

In this section, the models for the two different types of UWB systems considered in this paper are presented. In each case, although the transmit signal is spread in such a way that multiple access can be accommodated, only a single user is assumed to be operating on the channel during the acquisition process. If multiple users were indeed present, the same results still can be applied exactly as long as the interference is assumed to be Gaussian and the operating signal-to-noise (SNR) ratio is modified appropriately. In addition to the basic transmit and receive signal models, some basics components of the hypothesis testing under each model are presented.

## 2.1 DS/SS System Model

Direct-sequence spread-spectrum (DS/SS) systems have found widespread use in a number of applications ranging from cellular telephony to wireless local area networks (WLANs). Recently, some have proffered DS/SS systems with a large spreading gain for application in UWB spectral allocations [10]. Hence, code acquisition for such systems is considered here; note that these acquisition schemes are also applicable, of course, to traditional DS/SS systems with large processing gains.

For the sake of simplicity and clarity, the following assumptions, which are similar to those made in [6], are made in the DS/SS system model:

1. The carrier frequency and phase are acquired prior to code acquisition.

2. No data is modulated during the acquisition process.

3. The phase of the spreading signal is an integer multiple of the chip width.

4. The chip timing is known to the receiver.

In many systems, some of these assumptions may be violated, so the algorithm derived below will need to be modified in a straightforward manner; however, the comparison of the performance of various search schemes given below should still hold approximately.

The desired "phase" of index $d$ is the (integer) offset in chips of the true start of the pseudonoise (PN) sequence from some arbitrarily chosen zero time for a PN period. The received equivalent baseband signal during the $n$th chip is:

$$r_n(t) = \sqrt{P} c_n^{(d)} g(t - nT_c) + n(t),\ nT_c \leq t \leq (n+1)T_c, \tag{1}$$

where $P$ is the received signal power, $g(t)$ represents the unit-amplitude rectangular chip waveform, assumed to be of duration $T_c$, $c_n^{(d)}$ is the value for this chip of the desired phase, and $n(t)$ is AWGN with two-sided power spectral density $\frac{N_0}{2}$. Unlike many DS/SS applications, the simplifying restriction to a rectangular waveform will not significantly change the results and hence is safely adopted. The goal of the acquisition is to determine this unknown correct phase $d$, which takes on some integer value between $0$ and the number of chips in one period of the PN sequence. For the DS/SS system, only this AWGN case will be considered.

At the receiver, a hybrid acquisition scheme will be employed. In particular, $M-1$ template signals with different phases are generated to correlate over some small period with the incoming signal. After normalization, the output of the $l$th correlator at time $(n+1)T_c$ is given by:

$$X_l(n) = \sqrt{\frac{2}{N_0 T_c}} \int_{nT_c}^{(n+1)T_c} r_n(t) c_n^{(d_l)} g(t - nT_c) dt \tag{2}$$

$$= p c_n^{(d)} c_n^{(d_l)} + W_l(n), \tag{3}$$

where $p = \sqrt{2PT_c/N_0}$, $d_l$ is the PN phase of the template signal of the $l$th correlator, and $\{W_l(n), n = 1, 2, \ldots\}$ are independent and identically distributed(i.i.d.) Gaussian random variables with zero mean and unit variance.

The correlator outputs are used in an $M$-ary hypothesis test. Let $\underline{X}(n)$ denote the vector of correlator outputs $(X_1(n), X_2(n), \ldots, X_{M-1}(n))^T$ at sample time $n$. Assuming the spreading sequence is a random binary sequence [6, 16], the $M$-ary hypothesis test in terms of the correlator outputs can be written as follows,

$$H_0 : \underline{X}(n) = p\underline{R}(n) + \underline{W}(n), \tag{4}$$

and for $k = 1, \ldots, M-1$,

$$H_k : \underline{X}(n) = p\underline{R_k}(n) + \underline{W}(n), \tag{5}$$

where elements of $\underline{R}(n)$ are i.i.d random variables taking values from $\{1, -1\}$ with equal probability; $\underline{R_k}(n)$ has the same distribution except the $k$-th element is 1; elements of $\underline{W}(n)$ are i.i.d Gaussian distributed random variables with zero mean and unit variance.

Therefore, the probability density function of $\underline{X}(n)$ under each hypothesis is given by:

$$H_0 : f_0(\underline{x}) = \prod_{i=1}^{M-1} \frac{1}{2\sqrt{2\pi}} \left[ e^{-\frac{(x_i-p)^2}{2}} + e^{-\frac{(x_i+p)^2}{2}} \right], \tag{6}$$

$$H_k : f_k(\underline{x}) = \frac{1}{\sqrt{2\pi}} e^{-\frac{(x_k-p)^2}{2}} \prod_{i=1, i\neq k}^{M-1} \frac{1}{2\sqrt{2\pi}} \left[ e^{-\frac{(x_i-p)^2}{2}} + e^{-\frac{(x_i+p)^2}{2}} \right], \tag{7}$$

where $\underline{x} \triangleq (x_1, x_2, \ldots, x_{M-1})^T$.

## 2.2 Impulse Radio Model

In a typical time-hopping spread-spectrum impulse radio system operating over a multipath fading channel, the received signal is

$$s_{rcv}(t) = \sum_{i=0}^{K-1} g_i s_{tr}(t - \tau_i) + n(t), \tag{8}$$

where $K$ is the number of multipaths, $\tau_i$ and $g_i$ are the delay time and gain for the $(i+1)$th path, respectively, $n(t)$ is zero-mean real-valued additive white Gaussian noise of two-sided power spectral density $\frac{N_0}{2}$, and the transmitted signal is given by [9]

$$s_{tr}(t) \;\; = \;\; \sum_{j=-\infty}^{\infty} \sqrt{E_p} p(t - jT_f - c_j T_c - \delta a_{\lfloor j/N_s \rfloor}), \tag{9}$$

where $p(t)$ is the transmitted pulse waveform with unit energy, which usually begins at time zero at the transmitter's clock, $E_p$ is the energy of a pulse, and $T_f$ is the frame time, which is typically a hundred to a thousand times the pulse width $T_m$. In order to avoid catastrophic collisions in multiple accessing, each user is assigned a distinct pseudorandom time-hopping (TH) sequence $\{c_j\}$ that multiplies $T_c$, which is the time shift parameter for the TH code. The TH sequence will have period $N_p$. The sequence $\{a_j\}_{j=-\infty}^{\infty}$ is the data stream of the desired user. Note, from (9), that the modulating data symbol changes only every $N_s$ frames.

Unlike synchronization in the DS/SS system, joint frame and TH code synchronization is required in UWB systems. To simplify the problem, some assumptions on the transmitted signal are made that do not influence the comparison of the performance of various sequential tests. The assumptions and their implication are as follows:

1. Interference from other users is ignored, and it is also assumed that there is no data transmission done by the transmitted signal during acquisition. Thus, the transmitted waveform has period $T_p = N_p T_f$, as is shown in Figure 2.

2. The chip time $T_c$ is equal to the pulse width $T_m$, and the frame time $T_f$ is assumed to be an integer multiple of such. Let $N_f = T_f / T_m$; then, the pseudorandom TH code is

a sequence of uniformly distributed random variables between 0 and $N_f - 1$. Thus, the pulse resides in any of the $N_f$ bins with equal probability.

3. The transmitted signal is assumed to only go through a single unfaded delay path or multiple equal-gain delay paths. The interval between the multipaths is the pulse width $T_m$. Acquisition of the phase corresponding to any of these paths can terminate the process.

4. The delay time is uniformly distributed in the interval $[0, N_p T_f]$.

With the above assumptions, now the problem is to determine the timing phase of the periodic transmitted waveform shown in Figure 2. Because of the continuity of the delay time, this acquisition problem is actually an estimation problem. However, the problem can be turned into a detection problem by assuming the delay time takes only discrete values at the receiver side. The total number of hypotheses then depends on the acquisition resolution, i.e. the unit delay time.

The template for a given correlator is a sequence of unit-amplitude pulses. At first glance, it appears that the hypothesis testing problem should then follow along the lines of the DS/SS framework in a straightforward manner. However, there are complications here. Due to the lack of frame timing, there may not be exactly one pulse in a given template waveform during a correlation period $T_f$ (see Figure 2). This greatly complicates the optimal test and requires some subtle design modification. Here, if there are two pulses in a given template during a correlation period $T_f$, only one will be correlated (i.e. the second is effectively removed from the template); if there is no pulse in a given template during a correlation period $T_f$, one pulse with random location in that period is added to the template. Moreover, pulses straddling frame boundaries are ignored. Hence, there is always one pulse in the template signal during a correlation interval. Let $s_{tm}^l(t)$ denote the template of the $l$th correlator. In the single-path channel, the output of the $l$th correlator at time $(n+1)T_f$ after normalization is given by

$$X_l(n) = \sqrt{\frac{2}{N_0}} \int_{nT_f}^{(n+1)T_f} s_{rv}(t) s_{tm}^l(t) dt \tag{10}$$

$$= p \sum_{j=J}^{J+1} \int_0^{T_f} p(t+(n-j)T_f - c_j T_c - \tau_0) p(t - \tau_{tm}^l) dt + W_l(n), \tag{11}$$

where $p = \sqrt{2E_p/N_0}$, $\tau_{tm}^l$ is the template pulse position within the frame, and $\{W_l(n), n = 1, 2, \ldots\}$ are i.i.d. Gaussian random variables with zero mean and unit variance. Because frame timing has not been acquired at this point, the integration period captures part of the period of each of two frames of the original transmitted signal; these frames are denoted with the indices $J$ and $J+1$ in (11). If there was no pulse in this frame and, hence, the template pulse position was randomly generated, this frame is effectively skipped by making the probability density function of the received signal under each hypothesis the same. Otherwise, if the phase of the template signal is correct, the output is

$$X_l(n) = p + W_l(n). \tag{12}$$

Assuming $\tau_{tm}^l$ to be a multiple of the pulse width $T_m$, the signal part of $X_l(n)$ takes the value 0 and $p$ with the probabilities $(N_f - 1)/N_f$ and $1/N_f$, respectively. Thus, the $M$ hypotheses are as follows in terms of the correlator outputs,

$$H_0 : \underline{X}(n) = p\underline{I}(n) + \underline{W}(n), \tag{13}$$

and, for $k = 1, \ldots, M-1$, if no random pulse is added to the template waveform of the $k$th correlator,

$$H_k : \underline{X}(n) = p\underline{I}_k(n) + \underline{W}(n), \tag{14}$$

otherwise,

$$H_k : \underline{X}(n) = p\underline{I}(n) + \underline{W}(n), \tag{15}$$

where elements of $\underline{I}(n)$ are i.i.d. taking values 0 and 1 with probabilities$(N_f - 1)/N_f$ and $1/N_f$ respectively; elements of $\underline{I}_k(n)$ have the same distribution except that the $k$th element is 1; elements of $\underline{W}(n)$ are i.i.d zero-mean Gaussian variables with unit variance, since the $M-1$ correlators correspond to different time slots.

Then, the probability density function of $\underline{X}(n)$ under each of the $M$ hypotheses can be given as follows. In all cases,

$$H_0 : f_0(\underline{x}) = \prod_{i=1}^{M-1} \frac{1}{N_f\sqrt{2\pi}} \left[e^{-\frac{(x_i-p)^2}{2}} + (N_f-1)e^{-\frac{x_i^2}{2}}\right]. \quad (16)$$

If no random pulse is added to the template waveform of the $k$th correlator,

$$H_k : f_k(\underline{x}) = \frac{1}{\sqrt{2\pi}} e^{-(x_k-p)^2/2} \prod_{i=1, i\neq k}^{M-1} \frac{1}{N_f\sqrt{2\pi}} \left[e^{-\frac{(x_i-p)^2}{2}} + (N_f-1)e^{-\frac{x_i^2}{2}}\right]; \quad (17)$$

otherwise, $f_k(\underline{x}) = f_0(\underline{x})$.

# 3 Derivation of the Algorithm

Assume that each of the $N$ possible phases is *a priori* equally likely. Per above, the first $M$-ary test will consider $M-1$ timing phases and a null hypothesis, which represents the remainder of the phases. Hence, the prior probabilities associated with the $M$ hypotheses for the first test are initialized as

$$\pi_0(0) = \frac{N-M+1}{N}$$
$$\pi_k(0) = \frac{1}{N}, \quad k = 1, \ldots, M-1$$

.

In the testing stage, the $M$-ary test can be an FSS test, MSPRT or RC-SPRT. Only hybrid acquisition based on the RC-SPRT is discussed in detail in this section, since algorithms based on the FSS and MSPRT are extensively discussed in [6]. One of the FSS tests is the *maximum a posterior probability* (MAP) test, which minimizes the overall error probability, but does not minimize the average acquisition time[6]. The decision rule of the MAP test is

$$\text{Decide } \; H_m \;\text{ if }\; m = \arg\max_j \left( \pi_j(0) \prod_{i=1}^{N} f_j(\underline{X}(i)) \right).$$

The only parameter to be be designed in this test is the sample size $N$.

The stopping time $N_A$ and final decision $\delta$ for the MSPRT, which is a sequential test, can be described as follows:

$$\begin{aligned} N_A &= \text{first } n \geq 1 \text{ such that } p_n^k > \frac{1}{1+A_k} \text{ for at least one } k, \\ \delta &= \arg\max_j p_{N_A}^j, \end{aligned}$$

where $p_n^k$ is the posterior probability - the probability of hypothesis $k$ given the data observed up through time $n$ (i.e. $p_n^k = P\{H = H_k \mid X_1, \ldots, X_n\}$). The parameters that need to be designed here are the constants $A_j$'s, which are positive and less than 1. Analytical optimal values of the thresholds in MSPRT and the sample size in MAP are difficult to obtain; hence, simulation is employed to determine these values. In hybrid acquisition based on the MAP and MSPRT, a choice of a single hypothesis is made at time $N$ or $N_A$, respectively. If that choice is of some $H_m$ for $m \neq 0$, this means that a timing phase has been chosen, and the acquisition process enters the verification process (see below). If that choice is $H_0$, the current group of phases are rejected and a new group of $M-1$ phases are introduced.

The stopping time $L_A$ and the decision of a basic RC-SPRT are described by

$$L_A = \min\{n \geq 0 : p_n^k < \frac{a}{a+1} \text{ for some k}\}, \tag{18}$$

$$\delta = \arg\min_k p_{L_A}^k, \tag{19}$$

where $p_n^k = P\{H = H_k \mid X_1, \ldots, X_n\}$ is the posterior probability, and the parameter $0 < a < 1$ is designed to minimize the expected acquisition time. Each time the test stops, only $H_\delta$, the hypothesis with the smallest posterior probability, is removed. If $\delta = 0$, the large composite hypothesis $H_0$ is the most unlikely hypothesis and will be removed, and new prior probabilities of the remaining hypotheses will be reassigned as follows

$$\pi_0(L_A+1) = 0, \tag{20}$$

$$\pi_j(L_A+1) = \frac{p^j_{L_A}}{\sum_{k=1}^{M-1} p^k_{L_A}}, j = 1, \ldots, M-1. \tag{21}$$

If $\delta \neq 0$ (the most commonly occurring case), the timing phase of the $\delta$-th correlator will be removed, and a new phase in the composite set $A(L_A)$ being considered under $H_0$ will replace the removed phase. Let $N(L_A)$ denote the number of phases in the composite set $A(L_A)$. Then the new set of prior probabilities of $M$ hypotheses will be reset as

$$\pi_j(L_A+1) = \frac{p^{(j)}_{L_A}}{\sum_{k=0,k\neq\delta}^{M-1} p^{(k)}_{L_A}},\ j = 1, \ldots, M-1, j \neq \delta, \tag{22}$$

and

$$\pi_0(L_A+1) = \frac{N(L_A)-1}{N(L_A)} \frac{p^{(0)}_{L_A}}{\sum_{k=0,k\neq\delta}^{M-1} p^{(k)}_{L_A}}, \tag{23}$$

$$\pi_\delta(L_A+1) = \frac{1}{N(L_A)-1}\pi_0(L_A+1). \tag{24}$$

The initial values are $N(1) = N - M + 1$ and $A(1) = \{d_M, d_{M+1}, \ldots, d_N\}$, respectively.

The number of hypotheses $N(n)$ in the composite hypothesis is set to zero if $\pi_0(n)$ is zero at any $n$. This happens when $H_0$ is rejected or the test has gone through all of the timing phases. When $N(L_A) = 0$, the new set of prior probabilities are

$$\pi_\delta(L_A+1) = 0, \tag{25}$$

$$\pi_j(L_A+1) = \frac{p^{(j)}_{L_A}}{\sum_{k=1,k\neq\delta}^{M-1} p^{(k)}_{L_A}},\ j = 1, \ldots, M-1, j \neq \delta. \tag{26}$$

In this case, the stopping rule for the succeeding stage has to be changed to

$$L_A = \min\{n \geq 0 : 0 < p^k_n < \frac{a}{a+1} \text{ for some k}\}, \tag{27}$$

$$\delta = \arg \min_{k, p^k_{L_A} \neq 0} p^k_{L_A}. \tag{28}$$

The basic test is repeated until only one simple hypothesis is left. During this final elimination process, the number of hypotheses under consideration will drop below $M$; in such a case, the prior set of probabilities after each drop is done according to (25) and (26) with obvious modifications to the indexing. When one simple hypothesis is left, that hypothesis is the final decision of the testing stage. Figure 3 is an illustration of RC-SPRT with three correlators.

For each of the testing schemes, the final decision is checked at the verification stage. If the phase is verified to be true, the acquisition process is complete. Otherwise, a new acquisition process has to be started again until the final decision at the testing stage is verified correct. The verification stage only uses one correlator and a binary FSS likelihood ratio test. The two hypotheses $H_0$ and $H_1$ represent respectively "the phase is correct" and "the phase is not correct". The verification process makes an error if it declares a correct phase to be incorrect or declares an incorrect phase to be correct. The sample size $T_v$ in the verification stage is chosen so that its error probability is negligibly small. In order for both types of error probabilities to be under $P_e$, the following has to be satisfied [6],

$$T_v \geq \frac{\log P_e}{\log[\min_\theta \rho(\theta)]}, \tag{29}$$

where $\theta > 0$, and

$$\rho(\theta) = \int_{-\infty}^{\infty} f_1(x)^\theta f_0(x)^{1-\theta} dx. \tag{30}$$

# 4 Analysis

The expected acquisition time is the criterion of performance in this paper. In [13], bounds on error probabilities and asymptotic expressions for the expected sample size and error probabilities of the MSPRT are given. In [14] [15], the asymptotic performance of a basic RC-SPRT was characterized when the error probabilities are very low and the expected sample sizes are very large. First, define the Kullback-Leibler(KL) distance between probability density functions $f_i$ and $f_j$ as follows,

$$D(f_i, f_j) \quad = \quad E_{f_i}\left[\log \frac{f_i(x)}{f_j(x)}\right]. \tag{31}$$

The asymptotic performance, in terms of average time to the conclusion of a test, of the MSPRT and the RC-SPRT, can be characterized by the following two formulas:

**MSPRT**

$$E_{f_k}[T] \longrightarrow \frac{-\log A_k}{\min_{j:j\neq k} D(f_k, f_j)} \; a.s. \quad \text{as } \max_l A_l \longrightarrow 0, \tag{32}$$

where $A_k$ is the threshold for $H_k$(see [13]).

**RC-SPRT**

$$E_{f_k}[T] \longrightarrow \frac{-\log a}{\max_{j:j\neq k} D(f_k, f_j)} \; a.s. \quad \text{as } a \longrightarrow 0. \tag{33}$$

Hence, the average time it takes the MSPRT to complete is inversely proportional to the KL distance to the *nearest* hypothesis from the correct one, whereas the average time it take the RC-SPRT to complete is inversely proportional to the KL distance to the *farthest* hypothesis from the correct one. This indicates that the RC-SPRT test will, on average, terminate much sooner than the MSPRT when there is a large difference in the KL distances from the correct hypothesis to the the closest and furthest hypotheses. However, of course, the MSPRT discards $M-1$ hypotheses when it terminates, whereas the RC-SPRT discards a single hypothesis.

By symmetry in the two UWB systems studied here, all hypotheses except the null hypothesis have the same KL distance to one another, and thus there is no advantage in average termination time for the RC-SPRT implied by (32) and (33). Moreover, as noted above, the RC-SPRT has to reject hypotheses one by one until one is left. This suggests that the RC-SPRT should provide a longer acquisition time than the MSPRT. However, numerical results in the next subsection do not support this conclusion. In [17], the authors point out that equation (32) only describes the behavior of the first term of the expansion for the expected sample size in the “asymmetric” situation, where for each hypothesis, the hypothesis with minimum KL distance to the correct hypothesis is unique. Also, it is believed that equation (33) does not characterize the asymptotic behavior of the RC-SPRT well in highly symmetric situations as considered here.

It is often of use to derive a general formula for the expected acquisition time in that it gives intuition into the performance of the acquisition process. Moreover, with this formula, direct simulation, which can be extremely time consuming in the highly spread systems of the UWB application, is not needed. Instead, parameters in the formula can be obtained through simpler simulations and the desired result can be obtained by substituting those parameters in the formula. The expected acquisition time for the single-path case (AWGN) will be derived. First, the necessary parameters are defined:

$A$: a basic RC-SPRT without the true hypothesis in the test,

$B$: a basic RC-SPRT with the true hypothesis in the test,

$C$: a composite RC-SPRT rejecting hypotheses until only one is left without the true hypothesis and the null hypothesis in the test,

$D$: a composite RC-SPRT rejecting hypotheses until only one is left with the true hypothesis in the test and the null hypothesis not in the test,

$V$ : verification stage,

$P_{i0}$ = $Pr$(reject any $H_i$, $i \neq 0 \mid H_0$),

$P_{00}$ = $Pr$(reject $H_0 \mid H_0$ ),

$P_{ij}$ = $Pr$(reject any $H_i$, $i \neq j \neq 0 | \; H_j$),

$P_{0j}$ = $Pr$(reject $H_0 \; | H_j$),

$P_{jj}$ = $Pr$(reject $H_j | \; H_j$),

$\hat{P_{ij}}$ = $Pr$(any $H_i$ is left at the end of the test, $i \neq j | H_j$, $H_0$ has been rejected),

$\hat{P_{jj}}$ = $Pr$($H_j$ is left at the end of the test$| \; H_j$,$H_0$ has been rejected).

Obviously,

$P_{00} + P_{i0} = 1$,

$P_{0j} + P_{ij} + P_{jj} = 1$,

$\hat{P_{ij}} + \hat{P_{jj}} = 1$.

The flow diagram of the proposed acquisition scheme is shown in Figure 4. With Mason's formula, the moment generating function is derived in a straightforward manner; then, using signal flow graph techniques presented in [18], the expression for the expected acquisition time is obtained. The result is given in the appendix with long and tedious derivations omitted. The expected acquisition time for FSS and MSPRT can be derived similarly (see [6]). The derivation of the expected acquisition time for the multipath case is very difficult, so direction simulation is the only way we have at this time to estimate the performance.

# 5 Numerical Results

In this section, the performance of the standard FSS MAP test, the MSPRT and the RC-SPRT are compared when they are used in DS/SS and impulse radio acquisition. Although analytical results in single-path cases can be obtained via the formulas derived in Section 4, all the data presented here are taken directly from simulation for the sake of consistency. The results are shown in Figures 5 through 11. For the DS/SS signal, the PN sequence is generated by the primitive polynomial 3023 (in octal notation) of degree 10. For the UWB signal, $N_f$, the ratio of the frame time to the monocycle width, is assumed to be 50, the period of the TH code is 32, and the acquisition resolution is $T_m/2$. Although the statistical model is based on the assumption that the acquisition resolution is $T_m$, the numerical results show it works very well with finer resolutions. The results in these figures are the optimal results, i.e. all parameters has been designed to minimize the expected acquisition time $E[T_{acq}]$ for each scheme. The sample size of the MAP test is optimized, and the stopping thresholds for MSPRT and RC-SPRT are optimized. The verification time is chosen to make the error probability of the verification stage to be less than $10^{-8}$. In the multipath case, the number of paths is $K = 9$, and the search strategy is "Look and Jump by K Bins" [19]. The units of the expected acquisition time in the figures are the chip width and frame width for the DS/SS and impulse radio, respectively.

The figures indicate that the RC-SPRT approach provides a much lower average acquisition time than the MSPRT and MAP approaches in the case that the number of correlators is large and the SNR is low. Noting that the SNR is defined in terms of the chip or pulse energy (i.e. this is the pre-despreading SNR or receiver input SNR), lower SNRs in the figures correspond to more highly spread systems as encountered in the UWB application, whereas higher SNRs correspond to signals with low-to-moderate spreading. Hence, the goal of reducing the acquisition time in highly spread systems has been achieved. At higher SNRs, the proposed scheme is inferior to previously proffered acquisition schemes. This loss in performance at higher SNR relative to the competitors was expected, since, in the higher SNR case, an obvious "winner" excels very quickly before all of the other hypotheses can be rejected by the RC-SPRT.

Finally, it is important to note that the three tests that are being compared are not of equal digital circuit complexity. In particular, the decision process for the fixed sample size (FSS) test is much simpler to implement than that for the MSPRT or the RC-SPRT. However, this decision process will be done digitally in UWB receivers, and hence will not be consume as valuable of a commodity as the analog correlation circuitry. In particular, integrated circuit technology continues to rapidly drive down the circuit cost of complex digital algorithms as implied by the MSPRT and RC-SPRT.

# 6 Conclusion

Exploiting the well-known tenet that advances in sequential detection theory can often be applied to produce gains in the acquisition of wideband spread-spectrum signals, this paper presents the adaptation of a recently-developed $M$-ary hypothesis testing approach (the RC-SPRT) of one of the authors to the acquisition of UWB signals. Unlike the original RC-SPRT test, which removed unlikely hypotheses rapidly to minimize metric computation in decoders, the test here replaces removed hypotheses with new candidates to minimize overall expected acquisition time. Numerical results for AWGN and multipath fading channels indicate that for high input SNRs, as would be appropriate in spread-spectrum systems with low to moderate processing gains, traditional fixed-sample size (FSS) tests or a previously-developed $M$-ary testing technique termed the MSPRT outperform the proposed technique. However, for cases where the input SNR is low and the number of correlators is large, as would be the case in the highly spread systems of the targeted UWB application, numerical results indicate a significant decrease in expected acquisition times through the proposed technique for both DS/SS and impulse radio systems.

# A Expected Stopping Time of the Proposed Test

Let $T_A$, $T_B$, $T_C$ and $T_D$ be the expected stopping times of the tests $A$, $B$, $C$ and $D$. Also let $T_v$ be the verification time. Then, the general formula for the expected acquisition time of the scheme based on the RC-SPRT is,

$$\begin{aligned} E\{T_{acq}\} &= \sum_{n=2}^{N-M+1} \frac{N'_n(1)D_n(1) - N_n(1)D'_n(1)}{ND_n^2(1)} \\ &\quad + \frac{M-1}{N} \frac{N'_1(1)D_1(1) - N_1(1)D'_1(1)}{D_1^2(1)} \end{aligned} \tag{34}$$

where

$$\begin{aligned} N_n(1) &= P_{i0}^{n-1}\hat{P}_{jj}\frac{1-P_{ij}^{N-M-n+2}}{1-P_{ij}}, \\ D_n(1) &= P_{i0}^{n-1}\left(1-\hat{P}_{ij}\frac{1-P_{ij}^{N-M-n+2}}{1-P_{ij}}\right. \\ &\quad \left. -P_{jj}\frac{1-P_{ij}^{N-M-n-1}}{1-P_{ij}}\right), \end{aligned}$$

$$\begin{aligned} N'_n(1) &= P_{i0}^{n-1}\hat{P}_{jj}[(n-1)T_A + T_B + T_D + T_v] \\ &\quad \frac{1-P_{ij}^{N-M-n+2}}{1-P_{ij}} + P_{i0}^{n-1}\hat{P}_{jj}(N-M-n \\ &\quad +1)P_{ij}^{N-M-n+1}T_B - P_{i0}^{n-1}\hat{P}_{jj}P_{0j}P_{ij}T_B \\ &\quad \left[\frac{(N-M-n+1)P_{ij}^{N-M-n}}{1-P_{ij}}\right. \\ &\quad \left. -\frac{1-P_{ij}^{N-M-n+1}}{(1-P_{ij})^2}\right], \end{aligned}$$

$$
\begin{aligned}
D_n'(1) &= (n-1)T_A P_{i0}^{n-1} - \frac{T_A P_{i0}(1-P_{i0}^{n-1})}{P_{00}} \\
&\quad -(T_A+T_C+T_v)(1-P_{i0}^{n-1}) - [(n-1)T_A \\
&\quad +T_B+T_D+T_v]\hat{P}_{ij}P_{i0}^{n-1}(P_{ij}^{N-M-n+1} \\
&\quad +\frac{1-P_{ij}^{N-M-n+1}}{1-P_{ij}}P_{0j}) - \hat{P}_{ij}P_{i0}^{n-1}P_{ij}T_B \\
&\quad \left[P_{0j}\frac{1-P_{ij}^{N-M-n+1}}{(1-P_{ij})^2}\right. \\
&\quad -\frac{(N-M-n+1)P_{0j}P_{ij}^{N-M-n}}{1-P_{ij}} \\
&\quad \left.+(N-M-n+1)P_{ij}^{N-M-n}\right] \\
&\quad -P_{jj}P_{i0}^{n-1}(nT_A+T_B+T_C+T_v) \\
&\quad \frac{1-P_{ij}^{N-M-n+1}}{1-P_{ij}} \\
&\quad -P_{i0}^{n-1}P_{jj}\left\{\frac{P_{i0}T_A}{P_{00}}\left[\frac{1-P_{ij}^{N-M-n}}{1-P_{ij}}\right.\right. \\
&\quad \left.+\frac{P_{ij}^{N-M-n}P_{i0}-P_{i0}^{N-M-n+1}}{P_{i0}-P_{ij}}\right] \\
&\quad +\frac{P_{ij}T_B(1-P_{ij}^{N-M-n})}{(1-P_{ij})^2} \\
&\quad \left.-\frac{(N-M-n)T_B P_{ij}^{N-M-n+1}}{(1-P_{ij})}\right\}.
\end{aligned}
$$

# References


[1] FCC First Report and Order: In the matter of Revision of Part 15 of the Commissions Rules Regarding Ultra-Wideband Transmission Systems, *FCC 0248*, April 2002.

[2] Multiband OFDM Alliance SIG, “MultiBand OFDM Physical Layer Proposal for IEEE 802.15 Task Group 3a, ” available at http://www.multibandofdm.org/.

[3] R. Kennedy, *Fading Dispersive Communication Channels.* New York: Wiley-Onterscience, 1969.

[4] I. Telatar and D. Tse, “Capacity and Mutual Information of Wideband Multipath Fading Channels,” *IEEE Transactions on Information Theory*, Vol. 46: pp. 1384-1400, July 2000.

[5] M. Medard and R. Gallager, “Bandwidth Scaling for Fading Multipath Channels,” *IEEE Transactions on Information Theory*, Vol. 48: pp. 840-852, April 2002.

[6] V. Veeravalli and C. Baum, "Hybrid acquisition of direct sequence CDMA signals," *International Journal of Wirless Information Network,* vol. 3, pp. 55-65, No. 1 1996.

[7] M. Zhu and K. M. Chugg, "Iterative message-passing algorithms for rapid PN code acquisition," *IEEE Conference on Military Communications(MILCOM),* Boston, MA, Nov. 2003.

[8] Y. Chao and R. Schultz, "Optimal and suboptimal receivers for ultra-wideband transmitted reference systems," *IEEE Global Telecommunications Conference(GLOBECOM),* San Fransico, CA, Dec. 2003.

[9] M. Win and R. Scholtz, "Ultra-wide bandwidth time-hopping spread-spectrum impulse radio for wireless multiple-access communications," *IEEE Transaction on Communications,* vol. 48, No. 4, Apr. 2000.

[10] P. Runkle, J. McCorkle, T. Miller and M. Welborn, "DS-CDMA: the modulation technology of choice for UWB communications," *IEEE Conference on Ultra Wideband Systems and Technologies,* Reston, VA, Nov. 2003.

[11] W. Lovelace and J. Townsend, "The Effects of Timing Jitter and Tracking on the Performance of Impulse Radio," *IEEE Journal on Selected Areas of Communications,* pp.1646-1651, vol. 20, no. 9, Dec. 2002.

[12] A. Wald, *Sequential Analysis*, New York: Wiley and Sons, 1947.

[13] C. Baum and V. Veeravalli, "A sequential procedure for multihypothesis testing," *IEEE Trans. on Inform. Theory,* vol.40, pp. 1994-2007, Nov. 1994.

[14] C. Kose, *Optimal Adaptive Transmitter and Receiver Techniques*, Master's Thesis, University of Massachusetts at Amherst, May 2000.

[15] C. Kose, D. Goeckel and S. Wei, "Minimum complexity sequential multihypothesis decision: theory and reduced complexity decoding," *International Symposium on Information Theory,* June 2001.

[16] K. K. Chawla and D. V. Sarwate, "Acquisition of PN sequences in chip synchronous DS/SS systems using a random sequence model and the SPRT," *IEEE Transaction on Communications,* vol. 42, no. 6, Jun 1994.

[17] V. Dragalin, A. Tartakovsky and V. Veeravalli, "Multihypothesis sequential probability ratio tests, part II: Accurate asymptotic expansions for the expected sample size," *IEEE Trans. Inform. Theory,* vol. 46, pp.1366-1383, July 2000.

[18] A. Polydoros and C. Weber, "A unified approach to serial search spread-spectrum code acquisition. I. II. , " *IEEE Trans. Commun.,*vol. COM-32, no.5, pp.542-549,May 1984.

[19] E. Homier and R. Scholtz, "Rapid acquisition of ultra-wideband signals in the dense multipath channel," *IEEE Conference on UWB Systems and Technologies,* Baltimore, MD, May 2002.

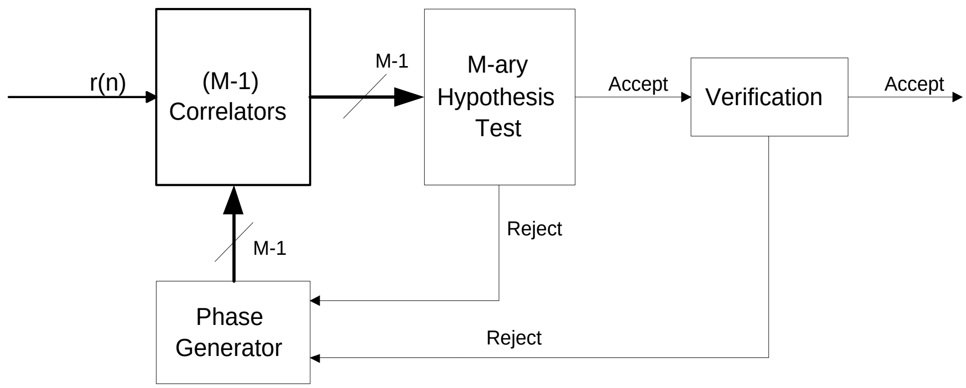


Figure 1: The structure of a standard hybrid acquisition scheme.

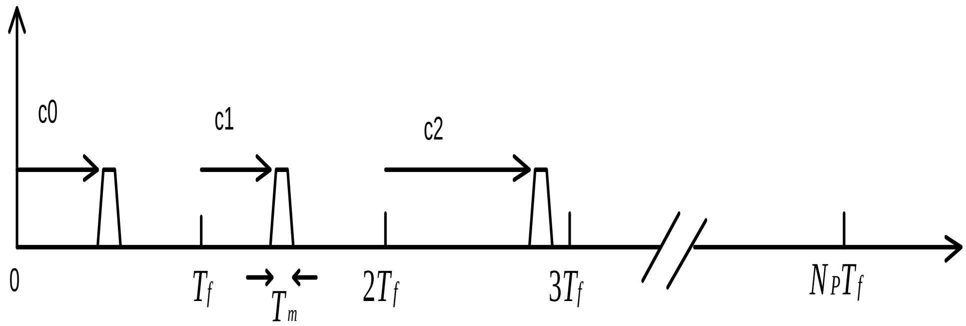


Figure 2: The waveform of an unmodulated impulse radio.

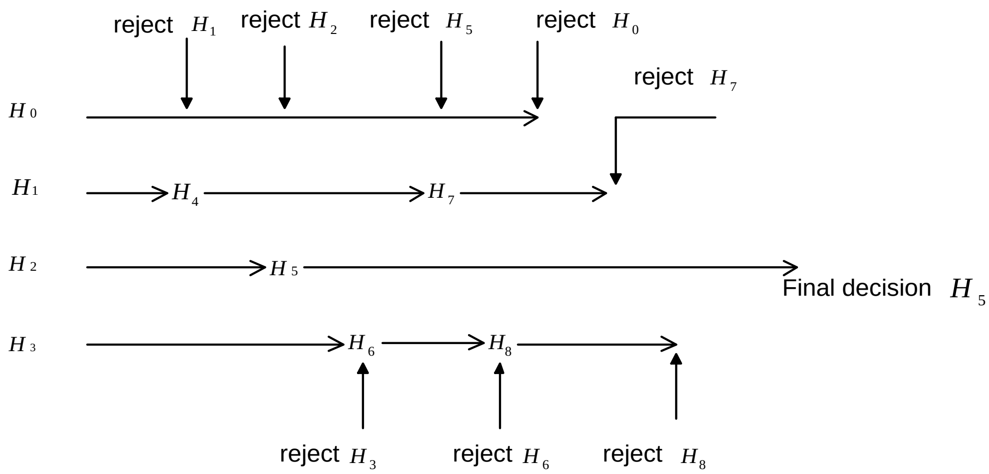


Figure 3: A simple example of the RC-SPRT operating on eight potential timing phases. Four hypotheses are considered together until one of them ($H_1$) becomes unlikely, at which time it is replaced with $H_4$. The process continues until all but one of the hypotheses has been eliminated, and this remaining hypothesis is the final decision.

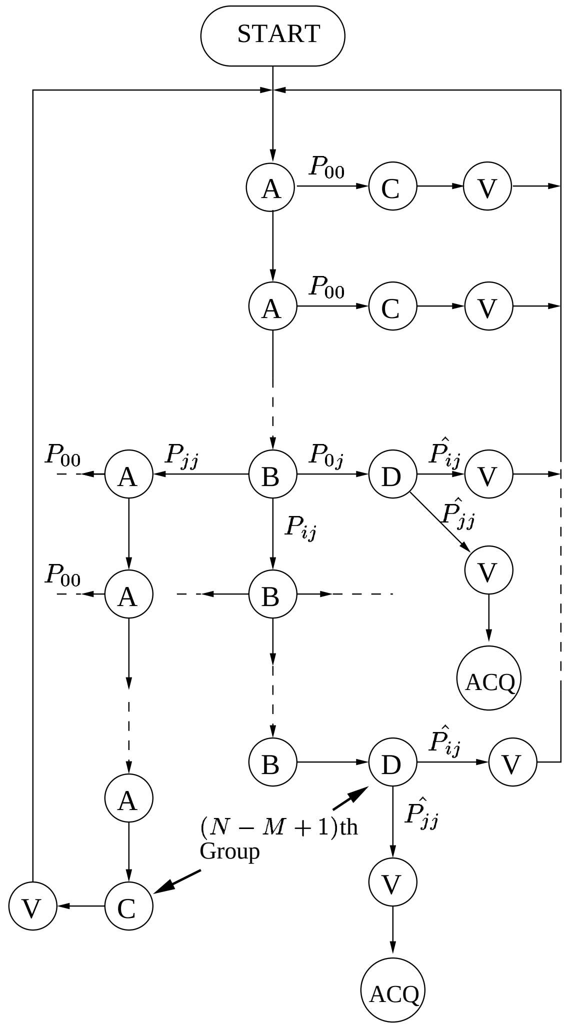


Figure 4: Flow diagram for the hybrid acquisition scheme based on RC-SPRT.

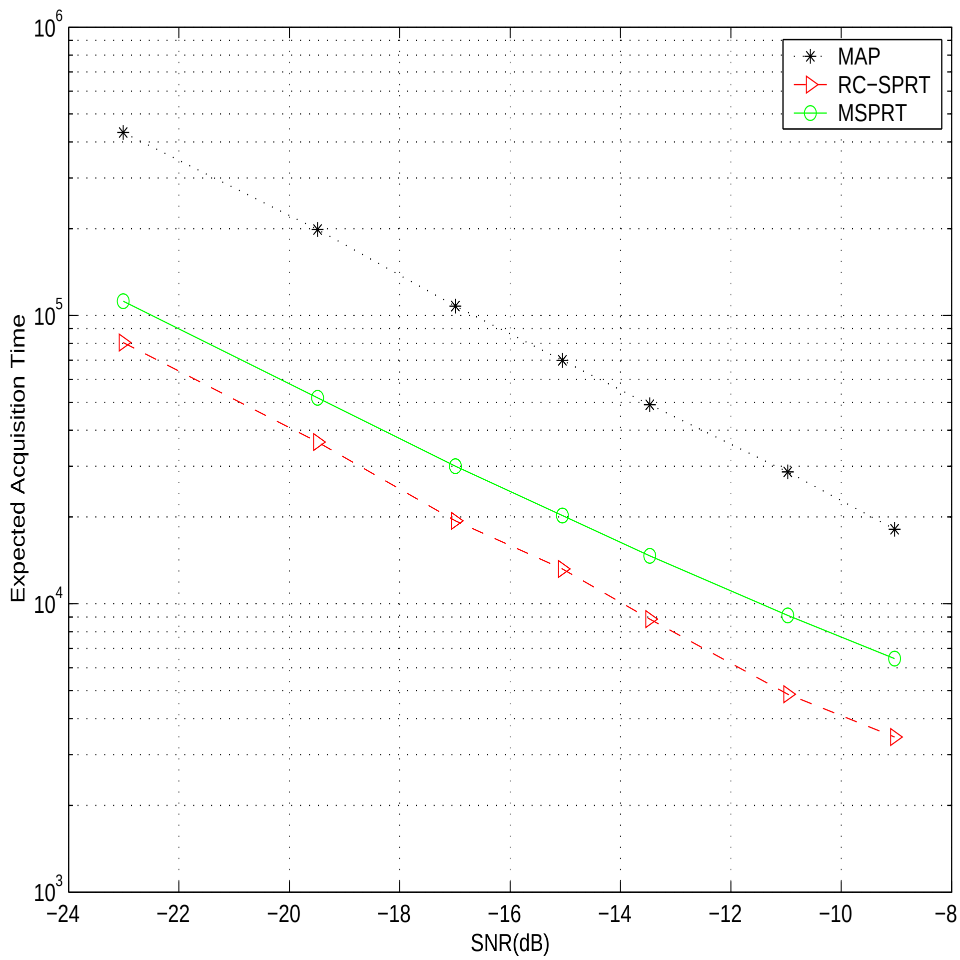


Figure 5: Expected acquisition time (in chips) of the hybrid acquisition schemes for DS/SS signals with $M = 4$ correlators. The PN sequence is generated by the primitive polynomial 3023 (in octal) of degree 10. In DS/SS systems, SNR is defined to be $PT_c/N_0$. Per the text, the signal-to-noise ratio (SNR) is defined per chip (i.e. the pre-despreading SNR). The post-despreading SNR at the decision point is larger by a factor of the processing gain; hence, operation at these very low SNRs, particularly for highly spread systems, is the norm. Observe that the RC-SPRT and MSPRT provide substantial gains over the FSS test, as expected, and that the improvement factor between RC-SPRT and MSPRT is roughly 1.5.

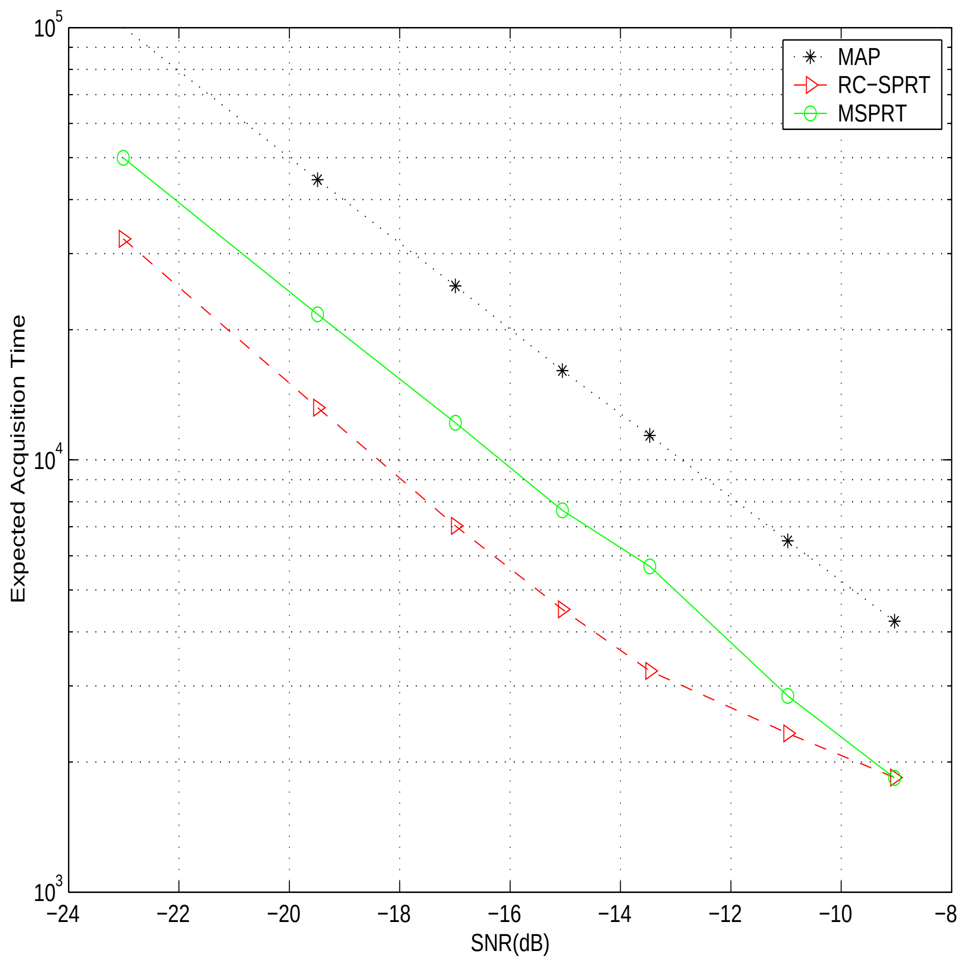


Figure 6: Expected acquisition time (in chips) of the hybrid acquisition schemes for DS/SS signals with $M = 20$ correlators, with the same system parameters as that characterized in Figure 5. The gains of the two sequential tests over the MAP decrease; however, the improvement factor between the RC-SPRT and MSPRT increases to about 2 for lower SNRs. Notice that the performances of the MSPRT and RC-SPRT merge at higher SNRs.

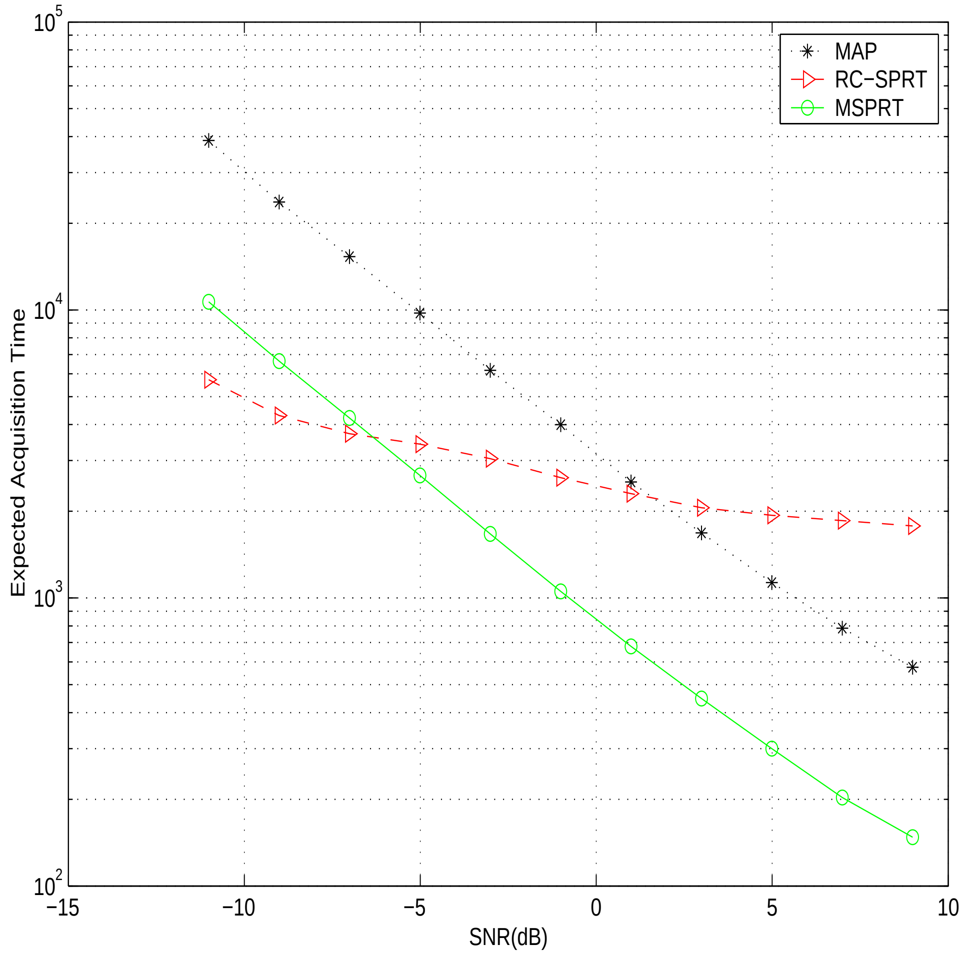


Figure 7: Expected acquisition time (in frames) of the hybrid acquisition schemes for impulse radio signals with $M = 20$ correlators. The system employs $N_f = 50$ frames per bit, a time-hopping code of period 32, and an acquisition resolution of one-half of the pulse width (i.e. $\frac{T_m}{2}$). In impulse radio systems, SNR $\triangleq E_p/N_0$. Per the text, the SNR is defined per impulse (i.e. the pre-despreading SNR). The post-despreading SNR at the decision point is larger by a factor of $N_s$; hence, operation at the lower of the SNRs shown, particularly for highly spread systems, is the norm. Observe that the acquisition time of the RC-SPRT does not decrease rapidly with increasing $E_p/N_0$ when $E_p/N_0$ is larger than -6 dB. With $E_p/N_0$ large enough, the MSPRT, even the MAP, eventually outperforms the RC-SPRT.

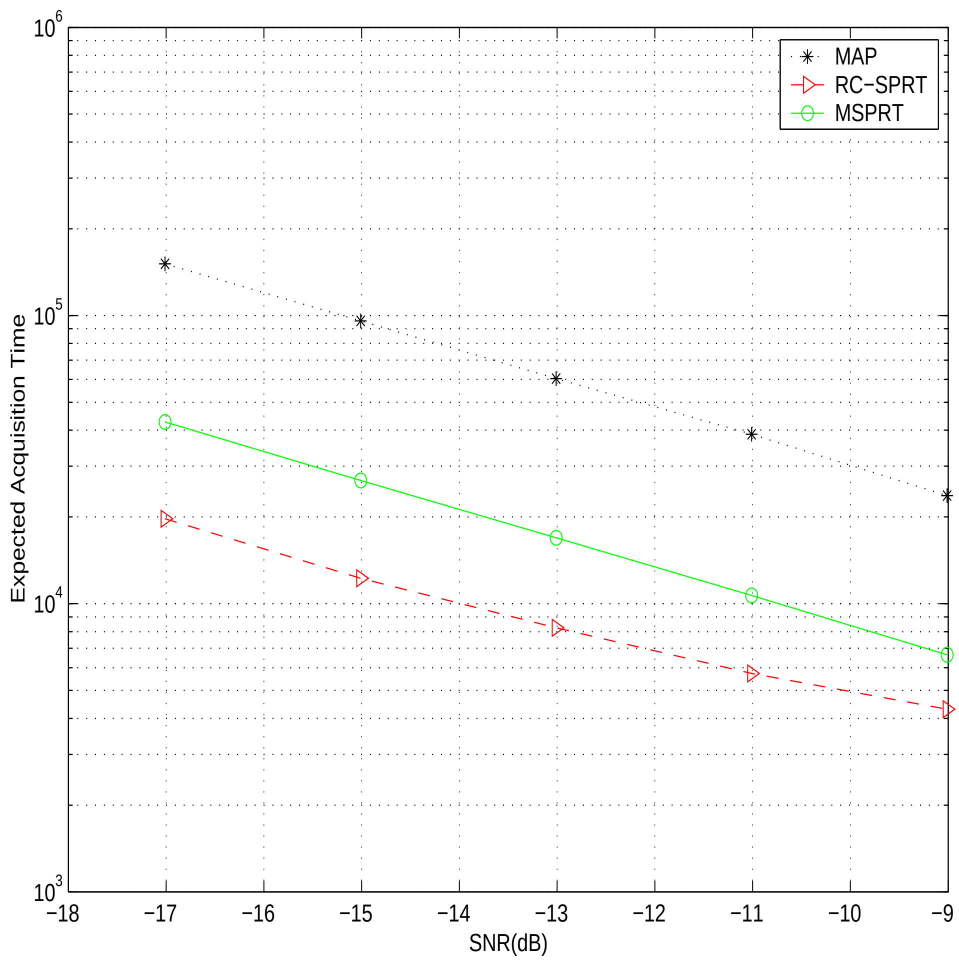


Figure 8: Expected acquisition time (in frames) of the hybrid acquisition schemes for impulse radio signals with $M = 20$ correlators and lower SNRs than those in Figure 7. The remainder of the system parameters are identical to those of the system characterized in Figure 7. Note that the RC-SPRT is 1.5 times and 8.5 times faster than the MSPRT and MAP, respectively, at these lower SNRs, with the ratios of the expected acquisition times for the various tests roughly independent of the SNR in this range.

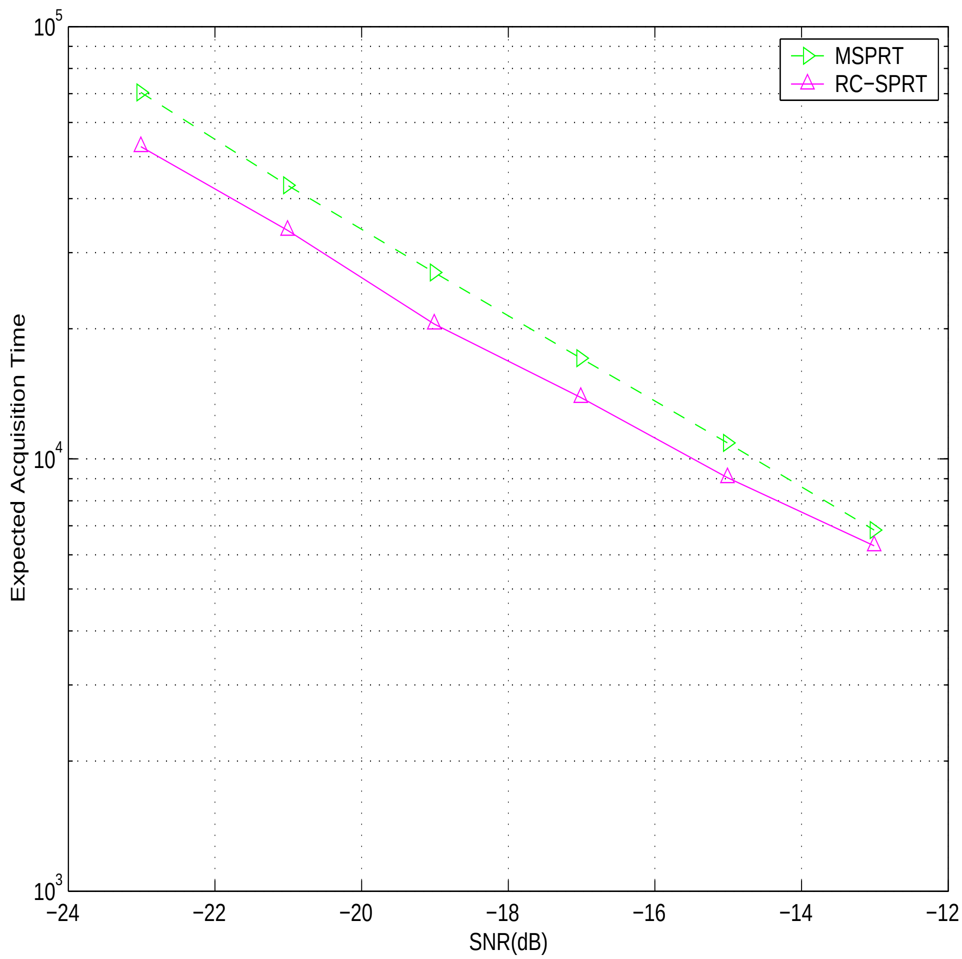


Figure 9: Expected acquisition time (in frames) of the hybrid acquisition schemes for impulse radio signals with $M = 4$ correlators in the multipath channel. The system parameters are identical to those of the system characterized in Figure 7, except that a multipath channel with $K = 9$ paths has been assumed. Appropriately, the SNR is now defined as $\frac{E_p}{KN_0}$ instead of $E_p/N_0$. Note that the RC-SPRT retains a 1.4 improvement factor versus the MSPRT.

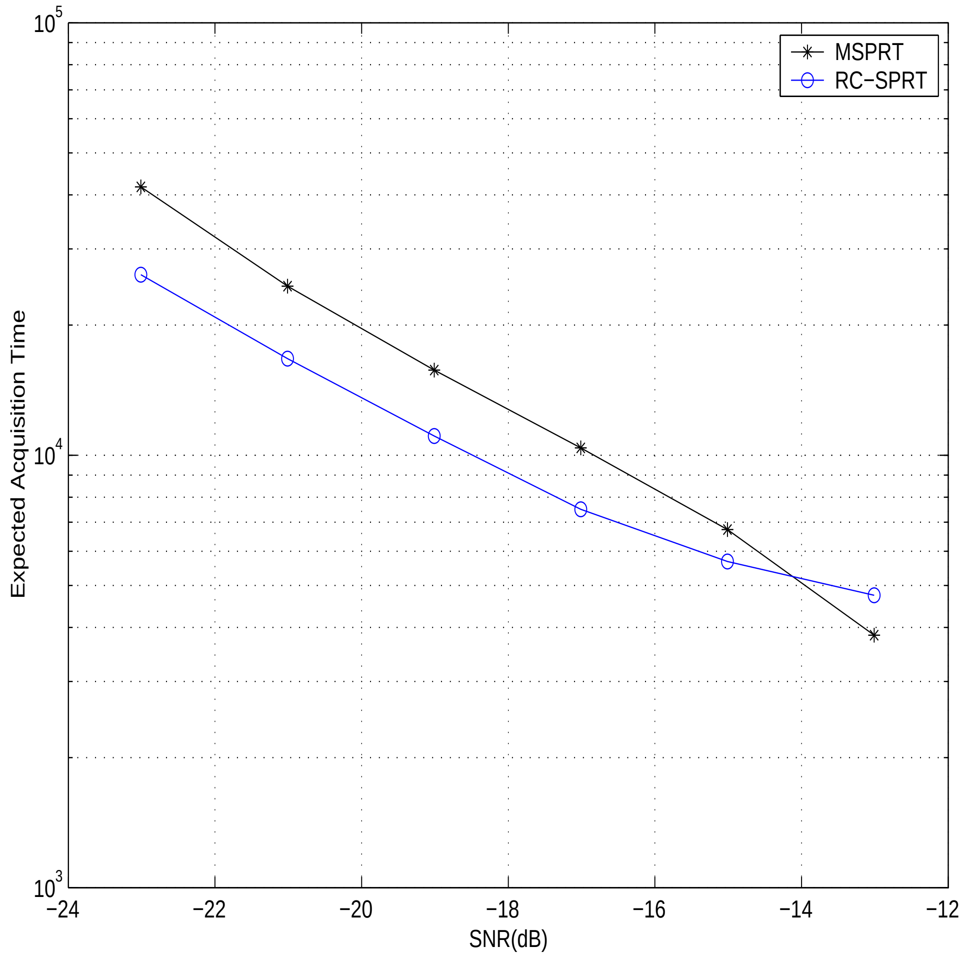


Figure 10: Expected acquisition time (in frames) of the hybrid acquisition schemes for impulse radio signals with $M = 20$ correlators in the multipath channel. The remaining system parameters are identical to those of the system characterized in Figure 9. Observe that the improvement factor is around 1.5 for SNRs less than -15dB.

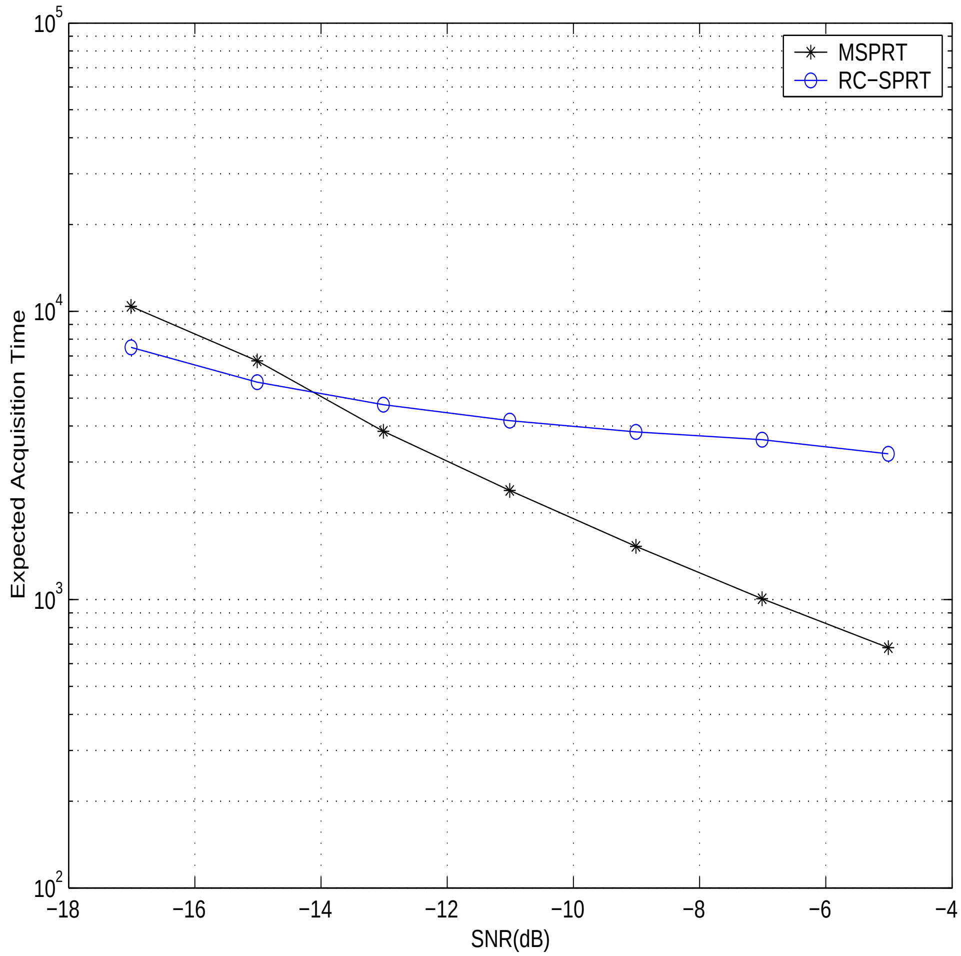


Figure 11: Expected acquisition time (in frames) of the hybrid acquisition schemes for impulse radio signals with $M = 20$ correlators in the multipath channel at higher SNRs. The remaining system parameters are identical to those of the system characterized in Figure 9. Conclusions on the relative merits of the tests are similar to those drawn for the AWGN channel.